Proceedings of ICRC 2001: 3238 © Copernicus Gesellschaft 2001

ICRC 2001

Evidence for acceleration of near-relativistic electrons by coronal shocks

D. Haggerty and E. Roelof

The Johns Hopkins University Applied Physics Laboratory

Abstract. The time histories of near-relativistic impulsive electron beam events (38-315 keV, $0.4 < v/c < 0.8$) measured at 1 AU provide unique information on their solar acceleration process. Nearly 80 such events have been identified by ACE/EPAM from 1997 through 2000. We have performed a detailed statistical analysis of the timing between the near-relativistic electron injection and the soft X-ray, microwave, metric type-III, and chromospheric Hα emission. We find that the 40-300 keV impulsive electron events observed at 1 AU are injected on average 10 minutes after the solar electromagnetic (EM) emissions. Consequently we rarely see 38-315 keV electron injections simultaneous with any solar electromagnetic emissions, including the metric type-III bursts (which are known to be created by low energy electron beams escaping the corona). Therefore the electron populations escaping at the time of the EM emissions must have a much softer spectrum than the 38-315 keV electron events that are injected at a later time.

1 Introduction

The initial in situ observations of non-relativistic electrons (Van Allen and Krimigis, 1965) and relativistic electrons (Cline and McDonald, 1968) were associated with solar electromagnetic emissions. Reviews of the non-relativistic (Lin 1974, 1985) and relativistic electrons (Simnett, 1974) showed that the impulsive electron events observed in interplanetary space are only loosely coupled with Hα flares, hard X-ray (HXR) events, microwave bursts, and even metric and decimetric type-III radio bursts (which are known to be produced by electrons escaping the sun into interplanetary space). The lack of timing agreement between impulsive near-relativistic electron beams observed in interplanetary space and detailed yet semi-uncorrelated observations of electromagnetic radiation (some produced by energetic electrons) emitted in the solar chromosphere and low corona represents a significant observational and theoretical challenge.

Adding to this challenge the origin are a number of reports of a delay between solar flare related electromagnetic emission and the most probable injection time of the relativistic electrons Simnett (1974), as well as a delay between the injection of the relativistic and non-relativistic electron populations themselves (Lin 1974, Svestka 1976). In this study we report that the near-relativistic electron populations (38-315 keV) observed 1997-2000 near 1 AU from the ACE spacecraft that show a median $\sim$10 minute delay between the emission of electromagnetic radiation and the injection of the near-relativistic electron populations.

Correspondence to: D. Haggerty
(Dennis.Haggerty@jhuapl.edu)

2 EPAM instrument

The EPAM instrument, Electron, Proton, and Alpha Monitor (Gold, 1998), is designed to make measurements of ions and electrons over a broad range of energy and intensity with five separate solid-state detector telescopes that provide nearly full coverage of the unit sphere. This study uses high-resolution electron data obtained by the EPAM instrument through two independent techniques.

The deflected electron (DE30) segment of the Low-Energy Magnetic Spectrometer (LEMS30) telescope measures electrons by magnetically deflecting the incoming electrons with energy below 315 keV into a solid-state detector. The LEMS30 telescope sweeps out an annulus centered at 30° (± 25°) to the anti-Earthward (Sunward) spin axis of the ACE spacecraft and data are accumulated in four 90° sectors each of 3 seconds duration. The DE system contains four electron channels between 38-315 keV.

The second telescope (LEFS60) uses an aluminized Parylene foil, nominally 0.35 mg cm^{-2} thick, to absorb ions with energies below approximately 350 keV, while allowing electrons with energies above 35 keV to pass through to a solid-state detector. The LEFS60 telescope samples an annulus centered at 60° (± 25°) to the ACE spin axis and has eight

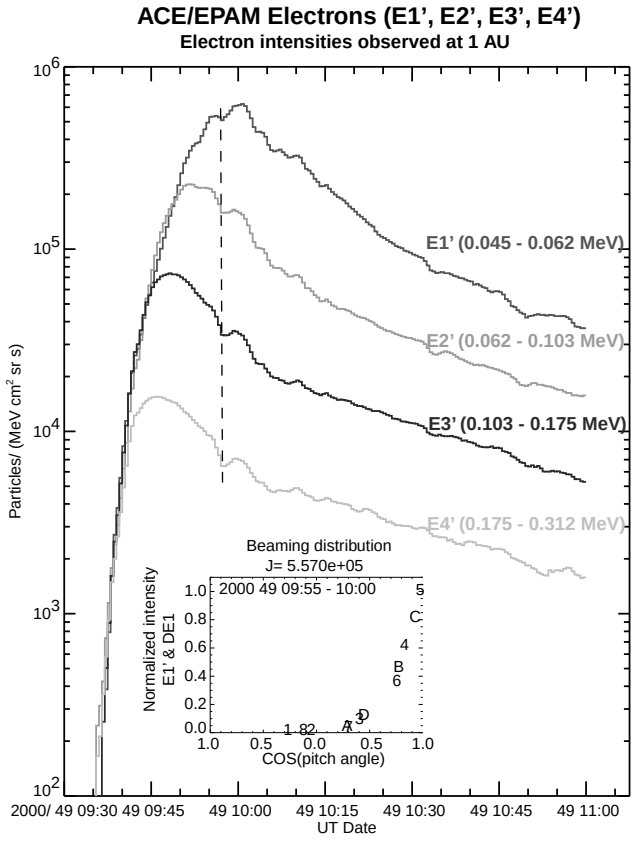

Fig. 1. Energetic electrons observed at 1 AU by ACE/EPAM. Intensity histograms at four energies and a representative pitch-angle distribution (labeled by detector spin sector).

45° sectors accumulating data at 1.5 seconds/sector. The LEFS60 system contains four electron channels between 45-312 keV.

3 Electron event list

From the launch of the ACE spacecraft (25 August 1997) through 9 September 2000, EPAM observed 267 energetic electron events above pre-existing intensity levels. For this study a minimum intensity of 10^3 particles/(cm^2 sr sec MeV) at 38-62 keV, was required for the identification of the electron event onsets with sufficient statistical confidence. Studies of these electron events at the highest temporal resolution show that many have isotropic pitch angle distributions or non dispersive spatial onsets. The remainder is composed of beaming distributions, with pitch angles highly collimated along the interplanetary magnetic field (IMF). With the goal of establishing the precise time that the near-relativistic electrons were injected into the heliosphere, only those events composed of beaming distributions with strong anisotropy were used because they are minimally affected by interplanetary propagation. From the initial 267 electron events, 79 (30%) were selected for this study based on the following two criteria.

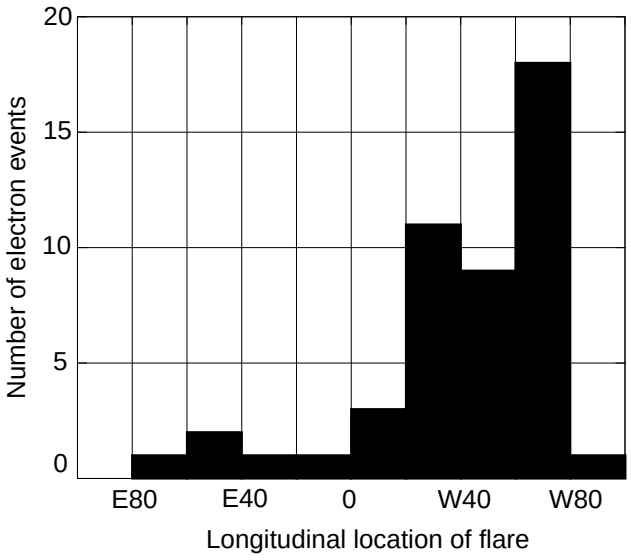

Fig. 2. Histogram showing longitude of chromospheric Hα flares associated with near-relativistic electron beam events observed at 1 AU. The event selection criteria results in well connected western events.

Clear electron onsets We define the onset time as the time when the electron intensity is first observed rising above the pre-event intensity. For our electron event list we used the time of the highest energy channel (i.e. highest velocity electrons) where a clear onset was observed. This minimizes the effect of wave/particle interactions en route to 1 AU (see below).

Beaming distributions A beaming distribution has two characteristics: (1) a clear anisotropic distribution during the rise phase while (2) the direction of the peak electron intensity remains closely aligned with the IMF. As the energetic electrons are accelerated and released onto open interplanetary field lines and stream outward into the heliosphere, those particles whose pitch angles remain close to the IMF during their outward transit will be observed first at 1 AU. Thus, it is imperative that those electrons whose path is along the IMF are used to establish the onset time. The energetic electron pitch angle distributions (PAD) are used to determine which electron events show a beaming distribution, which detector system and direction (sector) measures the pitch angle most nearly parallel to the IMF, and therefore which system (LEFS60 or DE30) should be used to establish a precise electron injection time.

The electron event shown in Figure 1 is representative of the 79 events included in this study. The pre-event electron intensity has been subtracted to highlight the clear and prompt onset. The peak electron intensities at different energies show clear velocity dispersion yet equal intensities in all channels are measured during the rising phase of the event. This flat energy spectrum is the signature of interplanetary wave-particle interactions Roelof (2000). The effect of interplanetary wave particle interactions is to make the observed onset the earliest possible arrival time for the energy mea-

sured at the spacecraft, so that the interaction has the least effect in the highest energy channel. The electron intensities began sharply rising at 0930 with the E'4 channel reaching a peak intensity near 0945 and the slower E'1 channel reaching a peak near 1000. A slight local interplanetary effect is identifiable by an intensity fluctuation not dispersed in time; it is marked by a dashed line just before 1000 UT.

A five-minute averaged electron pitch angle distribution (PAD) at the bottom of Figure 1 shows E'1 electrons (8 spin sectors labeled 1-8) as well as DE1 electrons (4 spin sectors labeled A-D). The energy coverage of the two systems is essentially the same. For each sector displayed in the PAD, the cosine of the electron pitch angle is plotted on the abscissa, and the intensity (normalized to the sector maximum) is plotted on the ordinate. The peak differential intensity (J) measured in particles/(cm^2 sr sec MeV) is indicated above the PAD. The peak of the distribution is clearly seen in sector 5 which is parallel to the magnetic field. The sectored angular distribution has a HWHM of $\sim$33° (cosine = 0.83). This HWHM is comparable to the opening angle of the collimator (24°), so the actual beam is probably as narrow, or even narrower than the collimator itself.

While most escaping electron events are observed at energies below $\sim$20 keV and are unassociated with chromospheric Hα flares, Lin (1993) found $>$60% of energetic electron events (E$>$15 keV) have an associated Hα flare. To verify that the electrons propagate directly along IMF lines once they were released into the interplanetary medium, we use the Hα location as a proxy for the location from where the electrons were released into the heliosphere. Of the 79 events, 60% had an associated chromospheric Hα flare reported in the Solar-Geophysical data. Figure 2 shows a histogram of the 47 events where an Hα flare location was reported. The vast majority of these events (37/47) are well connected to W30°-W70°.

4 Solar electromagnetic emission correlations

The NOAA Solar-Geophysical data archive contains the timing of the electromagnetic emission from the low corona. In this study we use the timing of the fixed frequency microwave bursts (RBR) at 8800 MHz and 15400 MHz, the sweep frequency (RSP) metric type III bursts, the soft X-ray events (XRA) and the chromospheric Hα flares (FLA) in comparison to the 79 electron events observed at 1 AU.

Figure 3 shows histograms that relate the timing of the energetic electron injections relative to various electromagnetic emissions. To compare the electron injection to the electromagnetic emission, the timing of all observations was taken back to the time of injection or emission. The injection time for the near-relativistic electrons was obtained from the onset of the highest energy electron channel where a clear event onset was observed and assuming 1.2 AU scatter free propagation along a Parker field (e.g., 13.7 minutes for a 235 keV electron). The electromagnetic emission time was obtained by subtracting 500 seconds from the earth received time to allow for propagation. In Figure 3 the time (t=0) corresponds to the electromagnetic emission and the histogram shows the release of the energetic electrons relative to that electromagnetic emission.

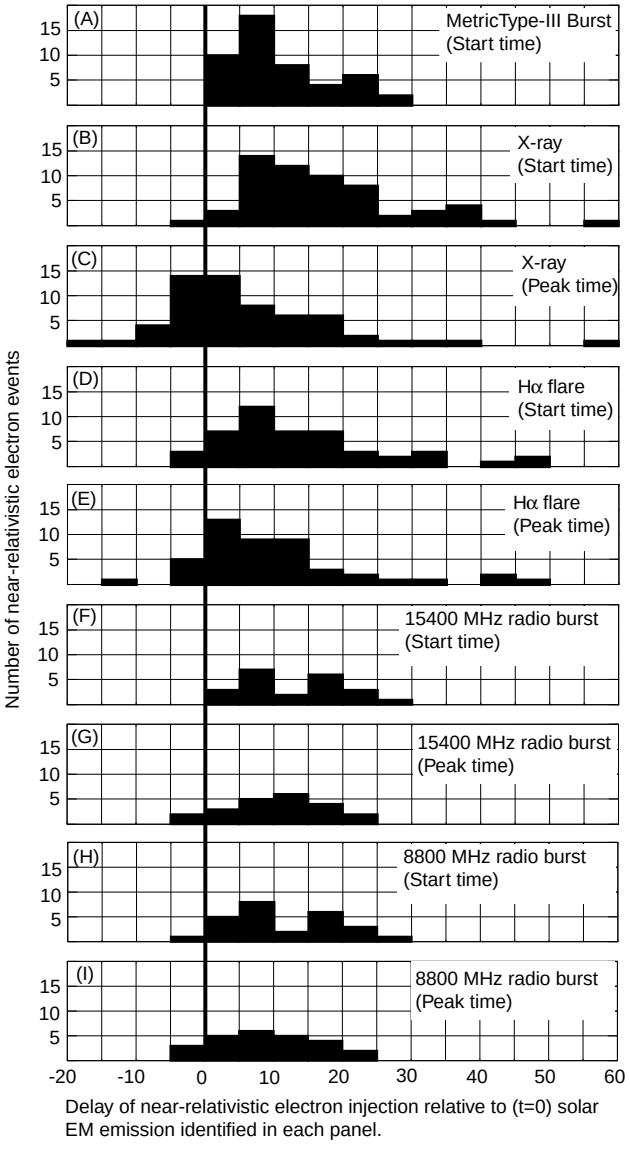

Fig. 3. Timing correlations between near-relativistic electron injection time and times of various electromagnetic emissions published in the Solar-Geophysical data (NOAA/SEL). A) metric type-III bursts, B)1-8 Å soft X-ray start time, C) 1-8 Å soft X-ray peak time. Panels D and E: Hα flare start and peak time respectively. Panels F and G: 15400 MHz microwave burst start and peak time, Panels H and I: 8800 MHz microwave burst start and peak time.

Of the 79 near-relativistic electron events in this study we found 45 metric type-III bursts that were clearly correlated with the energetic electron events. The comparison between the metric type-III emission and the near-relativistic electron injection is shown in Panel A of Figure 3. The electron injection is clearly delayed relative to the type-III emission by a median 9.5 minutes. A clear delay is also observed when compared to the chromospheric Hα flare start and peak

times. There is a median 12 minute delay compared to the Hα start time (Panel D) and a median 9 minute delay compared to the peak time (Panel E).

The best correlations between energetic electron events observed at 1 AU and solar electromagnetic emissions reported in the Solar-Geophysical data is with the GOES soft X-ray (SXR) events. We found 62 SXR events that were correlated with the energetic electron events. The delay between the energetic electron emission and the start and peak times of the SXR emission is seen in Panels B and C. A median delay of 15 minutes is observed compared to the SXR start time and a median delay of 4 minutes compared to the SXR peak time, even though some SXR events began a few minutes before the electron injection. The timing between microwave radio events and HXR emission is known to differ by less then one second and are well correlated (Aschwanden, 1995). We can therefore take the microwave emission time as a proxy for the electron-produced HXR event which occurs in the initial phase of the solar flare process. Energetic electrons are delayed by a median 14 minutes relative to the 15400 MHz microwave burst start time (F) and delayed by a median 11 minutes when compared to the peak time (G). There are 10 and 9 minute median delays observed relative to the 8800 MHz microwave start (H) and peak (I) times respectively.

5 Discussion and Conclusions

Timing correlations between HXR events, microwave bursts, chromospheric Hα flares, and metric type-III events have shown delays on the order of seconds or less. Studies of the so-called "second step" or "second phase" acceleration process found the characteristic time for acceleration is on the order of the transit time of a shock through a solar flare loop Bai (1979), Bai (1985), i.e. tens of seconds. This study clearly shows that the delay between the injection of near-relativistic electrons and all classes of electromagnetic emission is on the order of 10 minutes. Hudson (1982) reported 5-20 minute delays between electron injection and various phases of a limb-occulted flare and interpreted the delays as the time it took the acceleration agent to travel across the solar disk from the flare site to the injection longitude of W 60°. Recently Krucker (1999) reported delays between energetic electron events observed at 1 AU and dekametric type-III events observed above 2 solar radii, and discussed the delay in the context of high altitude EIT waves traveling from the flare site to the escape region.

In this study we have examined 79 impulsive near-relativistic electron events, the majority of which originated between W30°-W70° where a good solar connection and therefore no significant delays due to longitudinal or latitudinal propagation of either electrons or EIT waves would be expected. Nonetheless a median 10 minute delay is observed between solar electromagnetic emission and the injection of the energetic electrons into the inner heliosphere. We therefore believe that the delay is due to vertical transport of the accelerating mechanism on the order of 10 minutes. A typical coronal shock (1000 km/sec) originating near the chromosphere and propagating radially upward through the solar corona takes $\sim$10 minutes to propagate 1 solar radius.

Acknowledgements. The work performed at the Johns Hopkins University Applied Physics Laboratory has been supported by NASA under Task 009 of Contract NAS5-97271.

References

Aschwanden M. J., M. L. Montello, B. R. Dennis. A. O. Benz, Sequences of correlated Hard X-ray and Type III bursts during solar flares, ApJ, 440, 394-406, 1995.

Bai, T. and B. Dennis, Characteristics of Gamma-Ray Line Flares, ApJ, 292, 699-715, 1985.

Bai, T. and R. Ramaty, Hard X-Ray Time Profiles and Acceleration Processes in Large Solar Flares, ApJ, 227, 1072-1081, 1979.

Cline, T. L. and McDonald, F. B., Relativistic Electrons from Solar Flares, Solar Phys, 5, 507, 1968.

Gold. R. E., S. M. Krimigis, S. E. Hawkins III, D. K. Haggerty, D. A. Lohr, E. Fiore, T. P. Armstrong, G. Holland, L. J. Lanzerotti, Electron, Proton, and Alpha Monitor on the Advanced Composition Explorer Spacecraft, Space Science Reviews, 86, 541, 1998.

Hudson, H. S., R. P. Lin, R. T. Stewart, Second-Stage Acceleration in A Limb-Occulted Flare, Solar Physics, 75, 245-261, 1982.

Krucker, S, D. E. Larson, R. P. Lin, B. J. Thompson, On the origin of Impulsive Electron Events Observed at 1 AU, ApJ, 519, 864-875, 1999.

Lin, R. P., Non-Relativistic Solar Electrons, Space Science Reviews, 16, 189-256, 1974.

Lin, R. P., Energetic Solar Electrons in the Interplanetary Medium, Solar Physics, 100, 537-561, 1985.

Lin, R. P., The Relationship Between Energetic Electrons Interacting at the Sun and Escaping to the Interplanetary Medium, Adv. Space. Res., 13 (9)265-(9)273, 1993.

Roelof, E. C., Injection Histories of Impulsive Solar Energetic Electron Events: Effects of Interplanetary Wave-Particle Interactions, Trans. Am. Geophys. U., 81, F953, 2000.

Simnett, G. M., Space Res., 13, 745, 1972.

Simnett, G. M., Relativistic electron events in interplanetary space, Space Science Reviews, 16, 275-323, 1974.

Svestka, Z., Solar Flares, published by D. Reidel Publishing Co., pp279-282, 1976

Van Allen, J. A., and S. M. Krimigis, Impulsive Emission of 40 keV electrons from the Sun, J. Geophys. Res., 70, 5737, 1965.